



MIT Open Access Articles

A CMOS Molecular Clock Probing 231.061-GHz Rotational Line of OCS with Sub-PPB Long-Term Stability and 66-MW DC Power

The MIT Faculty has made this article openly available. **Please share** how this access benefits you. Your story matters.

| | |
|-----------------------|--|
| Citation | Wang, Cheng, Yi, Xiang, Kim, Mina, Zhang, Yaqing and Han, Ruonan. 2018. "A CMOS Molecular Clock Probing 231.061-GHz Rotational Line of OCS with Sub-PPB Long-Term Stability and 66-MW DC Power." |
| As Published | 10.1109/vlsic.2018.8502271 |
| Publisher | IEEE |
| Version | Author's final manuscript |
| Citable link | https://hdl.handle.net/1721.1/137635 |
| Terms of Use | Creative Commons Attribution-Noncommercial-Share Alike |
| Detailed Terms | http://creativecommons.org/licenses/by-nc-sa/4.0/ |

A CMOS Molecular Clock Probing 231.061-GHz Rotational Line of OCS with Sub-ppb Long-Term Stability and 66-mW DC Power

Cheng Wang*, Xiang Yi, Mina Kim, Yaqing Zhang and Ruonan Han

Massachusetts Institute of Technology, Cambridge, MA, US *Email: wangch87@mit.edu

Abstract

Recent progress of on-chip spectroscopic systems enables a new set of highly-stable frequency references (i.e. clocks) with low cost, power and volume. It is based on the rotational spectrum of gaseous molecules in sub-THz regime, a physical mechanism alternative to that in traditional atomic clocks. This scheme also enables fast start-up operation and robustness against mechanical vibration and external electromagnetic fields. This paper demonstrates the first chip-scale molecular clock in 65nm CMOS which probes the 231.061GHz spectral line of Carbonyl Sulfide ($^{16}\text{O}^{12}\text{C}^{32}\text{S}$). The clock consumes only 66mW DC power and has a measured Allan deviation of 3.8×10^{-10} with an averaging time of $\tau=10^3\text{s}$.

Introduction

Stable frequency references are critical for equipment used in navigation, communication and sensing. The widely adopted mechanical-resonance oscillators, such as crystal oscillator and MEMS oscillator, suffer from long-term frequency drifts due to external disturbances (vibration, temperature change, etc.) and aging. By optically probing the invariant electron transition of atoms, an atomic clock significantly improves the long-term stability. Chip-scale atomic clock (CSAC) further achieves clock miniaturization using coherent population trapping (CPT) [1, 2], but has exceedingly high cost and hence limited applications. Here, we show that sub-THz rotational spectral lines of gaseous molecules are a promising set of timebase for portable clocks. Compared to cesium (Cs) atomic clocks, our selected OCS molecular spectral line does not require the slow and power-consuming heaters for alkali evaporation, and is by nature less sensitive to external electromagnetic fields (e.g. Zeeman-shift coefficient is 98ppt/Gauss for OCS at 231.060983GHz and 150ppb/Gauss for Cs at 9.1926GHz). Thus, lower power, instantaneous start-up and better long-term stability are enabled. Its absolute linewidth $100\sim 1000\times$ larger than that in CSACs also leads to a high clock loop bandwidth of ~ 100 kHz, providing error corrections under rapid mechanical vibration. More importantly, this scheme, combined with recent progress in on-chip THz spectrometers [3], allows for clock implementation on low-cost silicon chips without any electro-optical assembly needed in atomic clocks. In this paper, we report the first molecular clock using a 65nm CMOS technology.

Architecture of Molecular Clock

The CMOS molecular clock is illustrated in Fig. 1. A rotational spectral line of OCS near $f_0=231.060983\text{GHz}$ is chosen. The OCS gas with 5-Pascal pressure is held inside a WR4.3 waveguide gas cell, the length ($L=140\text{mm}$) of which is optimized for maximum spectroscopic signal-to-noise ratio (SNR) [4]. Fig. 1 also presents the measured spectral profile with a quality factor of $Q=2.6 \times 10^5$. The Tx probing signal ($f_c \approx 231.061\text{GHz}$) is FSK-modulated (modulation frequency $f_m=16\text{kHz}$ and frequency deviation $\Delta f=1\text{MHz}$) and detected by a square-law detector in Rx. The intensity of two sidebands of

the FSK signal is shaped by the absorption line profile, and any frequency offset ($f_c - f_0$) leads to absorption imbalance and causes envelope fluctuation (at f_m) of the detector output. A feedback error voltage is then generated, which indicates the sign and magnitude of the frequency offset. After amplification and low-pass filtering, it is fed into a voltage-controlled crystal oscillator (VCXO) in the Tx to establish a dynamic frequency compensation for its 80-MHz output.

Probing Signal Generation and Detection on CMOS

Fig. 2 shows the Tx including a 224~242GHz fractional-N phase-locked loop (PLL). The sub-THz signal is extracted from a frequency quadrupler chain, which utilizes the nonlinearity of MOSFETs driven by a 57.8GHz harmonic oscillator. A 40-bit MASH 1-1-1 Δ - Σ modulator enables ppt-level frequency tuning resolution. The FSK modulation is performed by periodically changing the control word of the Δ - Σ modulator. The f_m and Δf of FSK are selectable with a resolution of 3-bit. Fig. 3 gives the schematic of the Rx. A NMOS transistor biased at sub-threshold is utilized as a square-law power detector. A low-noise folded-cascode op-amp further amplifies the baseband signal. Finally, the error signal is detected by an on-chip lock-in detector, which is referenced to f_m . To couple the probing signal from/into the chips, a pair of custom-designed chip-to-waveguide transitions using quartz probes is implemented. The loop filter is off-chip for post-fabrication adjustments of loop parameters.

Measurement Results

The measured loss of the gas cell is 7.3dB (Fig. 5 (left)). Fig. 5 (right) presents the output spectrum (no FSK) of the Tx at 231.061GHz. The output power including the loss of chip-to-waveguide transition ($\sim 10\text{dB}$) is -20.2dBm (Fig. 6). This power level avoids spectral broadening due to saturation [4]. The measured phase noise is -68.4dBc/Hz with a frequency offset of 1MHz. The measured noise equivalent power (NEP) of the Rx, including the transition loss, is $501\text{pW/Hz}^{0.5}$ at $f_m=16\text{kHz}$ (Fig. 6). Fig. 7 shows the packaged CMOS molecular clock as well as the dispersion curve (V_{error} versus f_c-f_0) measured by the FSK signal (in an open loop) with a SNR of 53dB. The molecular clock is locked onto the zero-crossing point of the curve. Fig. 8 (left) presents the measured instantaneous frequencies of the closed-loop clock and the free-running VCXO over 4000s. The measured stability (quantified by Allan deviation [5]) reaches 2.4×10^{-9} for $\tau=1\text{s}$ and 3.8×10^{-10} for $\tau=10^3\text{s}$. The suppression factor of VCXO frequency drift is $\sim 10\times$ through the molecular-clock regulation, and is expected to be higher under large ambient-temperature change. Shown in Table I, the CMOS clock achieves high stability (comparable to that in [1]), faster response (thanks to the much larger absolute linewidth), start-up speed, and significantly simplified construction. Currently, the drift of our prototype is mainly due to the OCS gas leakage of the set up (0.1Pascal/hr), which can be improved with a hermetic package. This, along with improved chip-waveguide transition design with reduced

loss (i.e. $\sim 10\times$ higher SNR), will lead to a predicted stability below 10^{-11} ($\tau=10^3$ s) (Fig. 8). The chip consumes 66mW power and the waveguide gas cell has a volume of 5.6cm^3 .

References

- [1] D. Ruffieux, et al., *JSSCC*, pp. 48-49, Feb. 2011.
- [2] Microsemi. QuantumTM, SA.54s chip scale atomic clock, 2017.
- [3] C. Wang, et al., *JSSC*, pp. 3361-3372, Dec. 2017.
- [4] C. H. Townes, *Microwave spectroscopy*, Courier Corp., 2013.
- [5] W. Riley, *Handbook of Freq. Stability Analysis*, NIST, 2008.

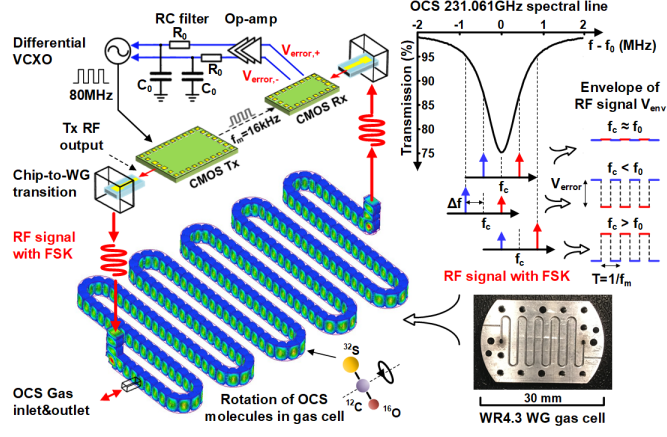


Fig. 1 System architecture of the molecular clock by probing the 231.061GHz OCS spectral line in a WR4.3 bended waveguide gas cell.

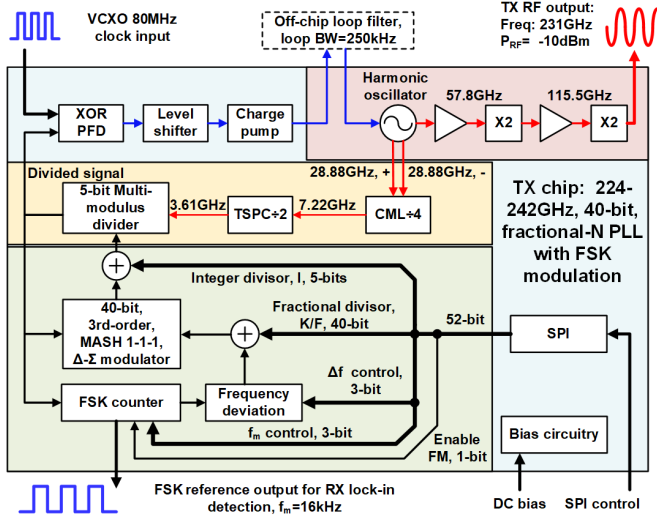


Fig. 2 Schematic of the clock Tx with a 40-bit fractional-N PLL.

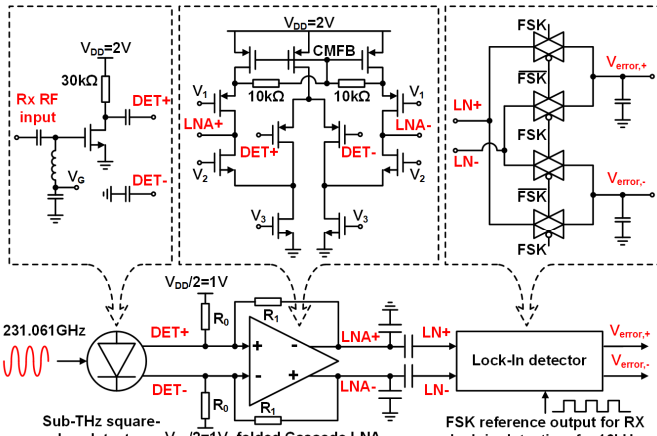


Fig. 3 Schematic of the clock Rx with THz and lock-in detectors.

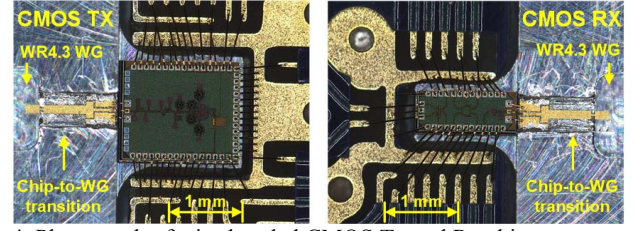


Fig. 4 Photograph of wire-bonded CMOS Tx and Rx chips.

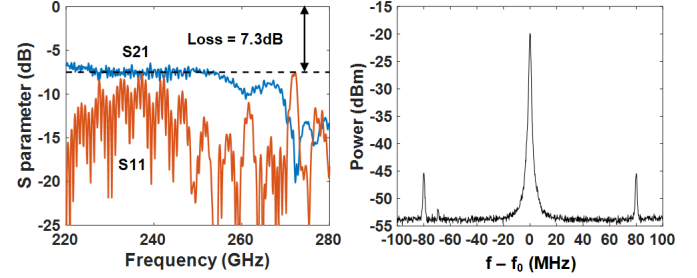


Fig. 5 The measured S-parameters of the waveguide gas cell (left) and the output spectrum of Tx at $f_0=231.010\text{GHz}$ (no FSK) (right).

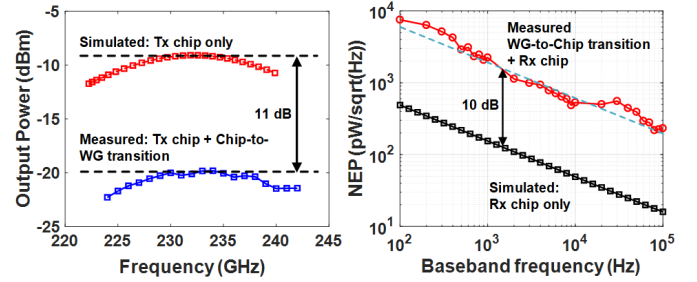


Fig. 6 The measured Tx output power at 224~242GHz (left) and the Rx noise equivalent power (NEP) at 231GHz (right).

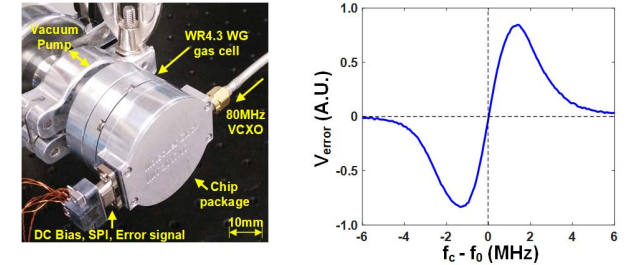


Fig. 7 Photograph of the packaged CMOS molecular clock (left) and the dispersion curve of the spectral line obtained by the chip (right).

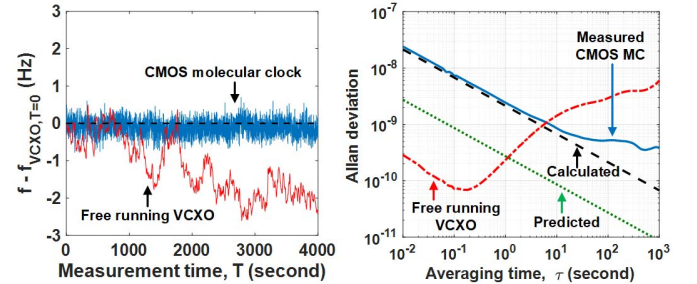


Fig. 8 Measured instantaneous frequency w/ and w/o locking (left) and the measured Allan deviation (right) using a Keysight 53230A counter.

TABLE I PERFORMANCE COMPARISON

| | Allan Deviation (10^3 s) | Linewidth (kHz) | $t_{\text{turn-on}}$ (second) | P_{dc} (mW) | Implementation |
|-----------|-----------------------------|-----------------|-------------------------------|----------------------|---------------------------|
| This Work | 3.8×10^{-10} | 880 | <1 | 66 ¹ | 65nm CMOS |
| CSAC [1] | 3×10^{-10} | ~ 1 | N/A | 26 ² | Electronics + Gas-Cell- |
| CSAC [2] | 1×10^{-11} | ~ 1 | 180 | 120 | Integrated Laser & Heater |

¹ The power of the VCXO is not included.

² The power of off-chip heater, laser, and other components is not included.